

Persistent X-Ray Photoconductivity and Percolation of Metallic Clusters in Charge-Ordered Manganites

D. Casa, V. Kiryukhin*, O.A. Saleh, and B. Keimer[†]

Dept. of Physics, Princeton University, Princeton, NJ 08544, USA, and

[†] Max-Planck-Institut für Festkörperforschung, D-70569 Stuttgart, Germany

J.P. Hill

Dept. of Physics, Brookhaven National Laboratory, Upton, NY 11973, USA

Y. Tomioka and Y. Tokura^{††}

Joint Research Center for Atom Technology (JRCAT), Tsukuba, Ibaraki 305, Japan, and

^{††} Dept. of Applied Physics, University of Tokyo, Tokyo 113, Japan

ABSTRACT

Charge-ordered manganites of composition $\text{Pr}_{1-x}(\text{Ca}_{1-y}\text{Sr}_y)_x\text{MnO}_3$ exhibit persistent photoconductivity upon exposure to x-rays. This is not always accompanied by a significant increase in the *number* of conduction electrons as predicted by conventional models of persistent photoconductivity. An analysis of the x-ray diffraction patterns and current-voltage characteristics shows that x-ray illumination results in a microscopically phase separated state in which charge-ordered insulating regions provide barriers against charge transport between metallic clusters. The dominant effect of x-ray illumination is to enhance the electron *mobility* by lowering or removing these barriers. A mechanism based on magnetic degrees of freedom is proposed.

PACS numbers: 72.40.+w, 71.30.+h, 72.80.Ga

* Present address: Dept. of Physics, 13-2154, MIT, Cambridge, MA 02139

The manganite perovskite $\text{Pr}_{0.7}\text{Ca}_{0.3}\text{MnO}_3$ has recently been shown to undergo an unusual insulator-metal transition when it is exposed to an x-ray beam [1]. Without x-rays, the material is semiconducting (with an average valence of +3.3 distributed uniformly over the Mn sites) at high temperatures, and charge-ordered insulating (with a static superlattice of Mn^{3+} and Mn^{4+} ions) below $\sim 200\text{K}$. Below $\sim 40\text{K}$, x-rays convert the insulating state to a metallic state which persists when the x-ray beam is switched off, but is removed on thermal cycling [1]. Interestingly, an equilibrium insulator-metal transition can also be induced by an external magnetic field [2], but not by irradiation with visible light. The material is, however, susceptible to dielectric breakdown at comparatively low electric fields [3] that can be triggered by laser light [4]. A microscopic explanation for this unusual behavior has thus far not been given. In this paper, we take the first steps in this direction by proposing a new mechanism for persistent photoconductivity (PPC), based on a quantitative analysis of new field and illumination dependent transport and diffraction data. Whereas a change in the *number* of conduction electrons is thought to be at the origin of PPC in conventional semiconductors, our data indicate that the electron *mobility* is the decisive factor in the manganites. The mobility is controlled mostly by magnetic degrees of freedom, that is, by the strong coupling of the conduction electrons (in the Mn e_g orbitals) to local spins (in the Mn t_{2g} orbitals) via Hund's rule.

The measurements were performed in a vertical-field superconducting magnet mounted on a two-circle goniometer at beamline X22B (photon energy 8 keV, flux $5 \times 10^{10}/\text{sec}$) at the National Synchrotron Light Source. An ion chamber was used to monitor the incident x-ray beam. The x-ray fluence (that is, the cumulative number of photons incident per mm^2 of sample surface) was estimated from the monitor counts. The diffracted beam was detected by a scintillation detector. The samples were single crystals of $\text{Pr}_{1-x}(\text{Ca}_{1-y}\text{Sr}_y)_x\text{MnO}_3$ synthesized by a floating zone method described previously [2]. The crystal surface was polished with diamond paste to better than $1 \mu\text{m}$. Two 4000 \AA thick Au electrical contacts about 2 mm apart were evaporated on a 200 \AA thick Cr buffer layer and annealed at 500°C for 10 hours. The contact resistance was less than 1Ω . The x-ray beam illuminated the region between the contact pads.

This experimental setup allows simultaneous measurements of the electrical conductivity and of the intensities of superstructure reflections characteristic of the cooperative Jahn-Teller distortion in the insulating state. These reflections occur at commensurate reciprocal lattice vectors (H, K/2, L), K odd, indexed on an orthorhombic lattice [1, 5, 6]. For reference, we have reproduced the central observations [1] on $\text{Pr}_{0.7}\text{Ca}_{0.3}\text{MnO}_3$ in Fig. 1a. The x-ray penetration depth is about $2 \mu\text{m}$, and the enhancement of the electrical

conductivity by several orders of magnitude shows that a thin metallic film is created on an insulating background when the material is exposed to x-rays (inset in Fig. 1). These metallic regions replace charge-ordered insulating regions, as indicated by the x-ray induced reduction of the superlattice peak intensity.

We have carried out a more comprehensive study of $\text{Pr}_{0.7}\text{Ca}_{0.3}\text{MnO}_3$ as well as analogous measurements on $\text{Pr}_{0.65}\text{Ca}_{0.245}\text{Sr}_{0.105}\text{MnO}_3$ and $\text{Pr}_{1-x}\text{Ca}_x\text{MnO}_3$ with $x=0.4$ and $x=0.5$, all of which exhibit charge ordering with the same wave vector as $\text{Pr}_{0.7}\text{Ca}_{0.3}\text{MnO}_3$. The average Mn valence for $x=0.5$ is 3.5, and a Mn^{3+} - Mn^{4+} superlattice with a doubled unit cell can form with a minimum number of defects. For $x=0.4$ and 0.3 , additional electrons have to be accommodated in defects or domain boundaries, and the charge-ordered lattice is less robust. This is reflected in the magnetic phase diagrams [2] which show that an external magnetic field induces a strongly first order insulator-metal transition associated with a large hysteresis region; progressively lower magnetic fields are required to induce this transition as x decreases. For the Sr-substituted compound, the critical field is even lower, and the metallic state reenters at low temperature even without application of a magnetic field. Some magnetic phase diagrams are reproduced in the insets of Fig. 1. As the charge-ordered lattice is antiferromagnetically ordered at low temperatures, defects and domain boundaries are expected to give rise to spin disorder.

While we observed an x-ray induced conductivity enhancement of the same order of magnitude as in $\text{Pr}_{0.7}\text{Ca}_{0.3}\text{MnO}_3$ in all of these compounds throughout most of the hysteresis region in the H-T phase diagrams (Fig. 1), a depression of the superlattice reflection was only observed in a narrower region close to the metallic side of the hysteresis region. An example is given in Fig. 1b for $\text{Pr}_{0.65}\text{Ca}_{0.245}\text{Sr}_{0.105}\text{MnO}_3$ where the peak intensity is independent of illumination at the 1% level. Note that in this compound the photoeffect occurs at a higher temperature where the intrinsic resistivity without x-rays ($\sim 10^3\Omega\text{cm}$) is much smaller than in $\text{Pr}_{0.7}\text{Ca}_{0.3}\text{MnO}_3$ at low temperatures ($> 10^6\Omega\text{cm}$). Since the resistance of the $2\ \mu\text{m}$ thick layer affected by the x-rays and the bulk of the crystal that remains unaffected are measured in parallel, the total x-ray induced resistance drop is much lower than in the $\text{Pr}_{0.7}\text{Ca}_{0.3}\text{MnO}_3$ experiment. The x-ray induced change in resistivity within the volume penetrated by the x-rays is comparable, however.

Closely similar observations were made in the other compounds, indicating that, despite the observations in $\text{Pr}_{0.7}\text{Ca}_{0.3}\text{MnO}_3$, persistent x-ray photoconductivity does not, *in general*, require the destruction of a significant amount of the charge-ordered phase. Rather, these new data suggest that substantial x-ray induced phase conversion, out of the charge-ordered insu-

lating phase, takes place only in a region of the phase diagram in which the metallic state is thermodynamically stable and the charge-ordered state is metastable. Since in $\text{Pr}_{0.65}\text{Ca}_{0.245}\text{Sr}_{0.105}\text{MnO}_3$, under the conditions of Fig. 1b, at most a very small amount of the charge-ordered phase is converted, the corresponding increase in the number of conduction electrons is also small, certainly much smaller than in $\text{Pr}_{0.7}\text{Ca}_{0.3}\text{MnO}_3$ (Fig. 1a). Nevertheless, both materials show comparable PPC. This observation is at odds with conventional models of PPC in semiconductors that rely exclusively on a photogenerated increase in the *number* of free charge carriers [8]. (According to these models, the carriers are photoexcited out of impurity states, and lattice relaxations prevent optical recapture.) By contrast, the decisive factor in the manganites appears to be the *mobility* of the electrons.

In order to elucidate how the x-ray photoelectrons affect the mobility of the charge carriers, we have carried out a systematic study of the current-voltage (I-V) characteristics in $\text{Pr}_{0.7}\text{Ca}_{0.3}\text{MnO}_3$. A synopsis of the evolution of the I-V curves with x-ray illumination in zero field, and with magnetic field after a brief x-ray exposure at $T=5\text{K}$, is given in Fig. 2. By repeating the magnetic field dependent measurements without x-ray exposure, we verified that for all curves of Fig. 2b the conductivity is dominated by the conducting film created by the initial brief x-ray illumination, with negligible contribution of the bulk of the crystal. Both sets of curves in Fig. 2 can thus be directly compared and, remarkably, turn out to be closely similar.

Whereas in both cases the transport is ohmic after prolonged x-ray exposure or in a high magnetic field, indicating a continuous metallic path between the contacts, the I-V characteristics are initially highly nonlinear. There are different possible origins of nonohmic conductivity in insulators, notably Joule heating, variable range hopping, and tunneling. The first two are ruled out by the nearly temperature independent conductivity below $T=10\text{K}$ shown in Fig. 3. Further, detailed consideration of the variable range hopping scenario [9] reveals that the electric fields at which such effects are predicted to become observable are several orders of magnitude larger than the weak fields applied here.

This leaves tunneling between x-ray induced isolated metallic islands as the only viable model. A surprisingly good fit to most curves can be obtained under the assumption that the transport is dominated by a small number of tunnel junctions in series, each of which is described by the well known Simmons model [10] with physically reasonable parameters (height of the insulating barrier $\sim 1 - 2\text{eV}$, thickness $\sim 10 - 30\text{\AA}$). These parameters are also consistent with those determined on a single trilayer manganite tunnel junction at comparable electric fields [11]. A typical result of such a comparison is shown in the inset of Fig. 3. A comprehensive analysis of all

I-V curves, including a possible special role of insulating barriers near the contacts, is beyond the scope of this paper.

The picture that emerges from this analysis is one in which a small number of insulating barriers act as “bottlenecks” for charge transport between the ferromagnetic metallic droplets. (Especially in narrow barriers, significant disorder may be present in both the charge ordering pattern and the antiferromagnetic spin alignment [6].) This explains why the x-ray induced enhancement of the conductivity is comparable in $\text{Pr}_{0.7}\text{Ca}_{0.3}\text{MnO}_3$ and $\text{Pr}_{0.65}\text{Ca}_{0.245}\text{Sr}_{0.105}\text{MnO}_3$ despite the vastly different number of conduction electrons added through phase conversion: The decisive step in both cases is an x-ray induced enhancement of the electron mobility by lowering or removing the insulating barriers. The parallel evolution of the I-V curves in Figs. 2a and b suggests that this proceeds in a very similar fashion upon x-ray illumination and upon application of a magnetic field. The effect of a magnetic field on these materials is much better understood than the effect of x-rays: In the generally accepted “double exchange” model, the field aligns the local t_{2g} spins ferromagnetically and facilitates hopping of the conduction electrons between adjacent Mn sites. This is believed to be the primary origin of the “colossal magnetoresistance” in the manganites. In the present case, the mobility through the barriers is enhanced if application of the field leads to canting of the local spins in the barriers. For a large enough field, some of the barriers may be entirely converted to the ferromagnetic phase so that adjacent metallic clusters coalesce. Fig. 2 suggests that these two effects (or a combination thereof) are also elicited by the x-rays. In $\text{Pr}_{0.65}\text{Ca}_{0.245}\text{Sr}_{0.105}\text{MnO}_3$, phase conversion is negligible (Fig. 1b) and the dominant effect has to be a modification of the spin alignment in the insulating barriers by the x-rays [12]. A possible mechanism involves penetration of the barriers (which are insulating to conduction electrons in the clusters) by hot x-ray photoelectrons which then actuate the double-exchange mechanism.

The importance of magnetic degrees of freedom in controlling the conductivity across the insulating barriers is underscored by I-V curves taken near the percolation threshold of the metallic clusters. Here, the I-V curves become unstable and exhibit frequent sudden jumps even for extremely low injected currents (Fig. 4). Interestingly, in the intermediate regime the behavior of the transport characteristics under x-ray exposure (Fig. 4a) and in a magnetic field (Fig. 4b) is systematically different. In the former case, jumps into states with higher and lower conductivity are approximately equally likely, while in the latter case, jumps occur exclusively into more highly conducting states.

This observation fits naturally into the above scenario in which the con-

ductivity near percolation is limited by tunneling through very narrow residual insulating regions with Mn atoms in metastable spin configurations. Local heating by a minute transport current allows these spins to explore different configurations. In the presence of an aligning field (Fig. 4b; the curves were taken with the magnetic field on), the final configurations are generally characterized by enhanced ferromagnetic correlation more conducive to charge transport. In the absence of an aligning field (Fig. 4a; the curves were taken with the x-ray beam off), there is no preferential spin alignment after the heating event, and the conductivity is equally likely to be reduced or enhanced. This demonstrates directly that nonequilibrium electrons can affect the mobility through the barriers by affecting their spin configuration.

In summary, we have identified a novel mechanism of PPC which is operative only for “hot” photoelectrons generated by high frequency radiation. Hot electrons appear to move an appreciable distance into the charge-ordered regions and enhance the electron mobility. The mechanism may involve a nonequilibrium carrier population near the top of the Mn e_g band that interacts with the local spins via double exchange. As electrons in the electric breakdown regime are also characterized by an effective temperature much higher than the crystalline environment, hot electron transport in these magnetically correlated materials provides a unified microscopic framework for both the photoinduced and the electric field induced insulator-metal transitions.

Acknowledgments. This work was supported by the National Science Foundation under grant No. DMR-9701991 (B.K.), by the Packard and Sloan Foundations (B.K.), by the US-DOE under contract No. DE-AC02-98CH10886 (J.P.H.), and by NEDO and Grants-In-Aid from the Ministry of Education, Japan (Y.T.).

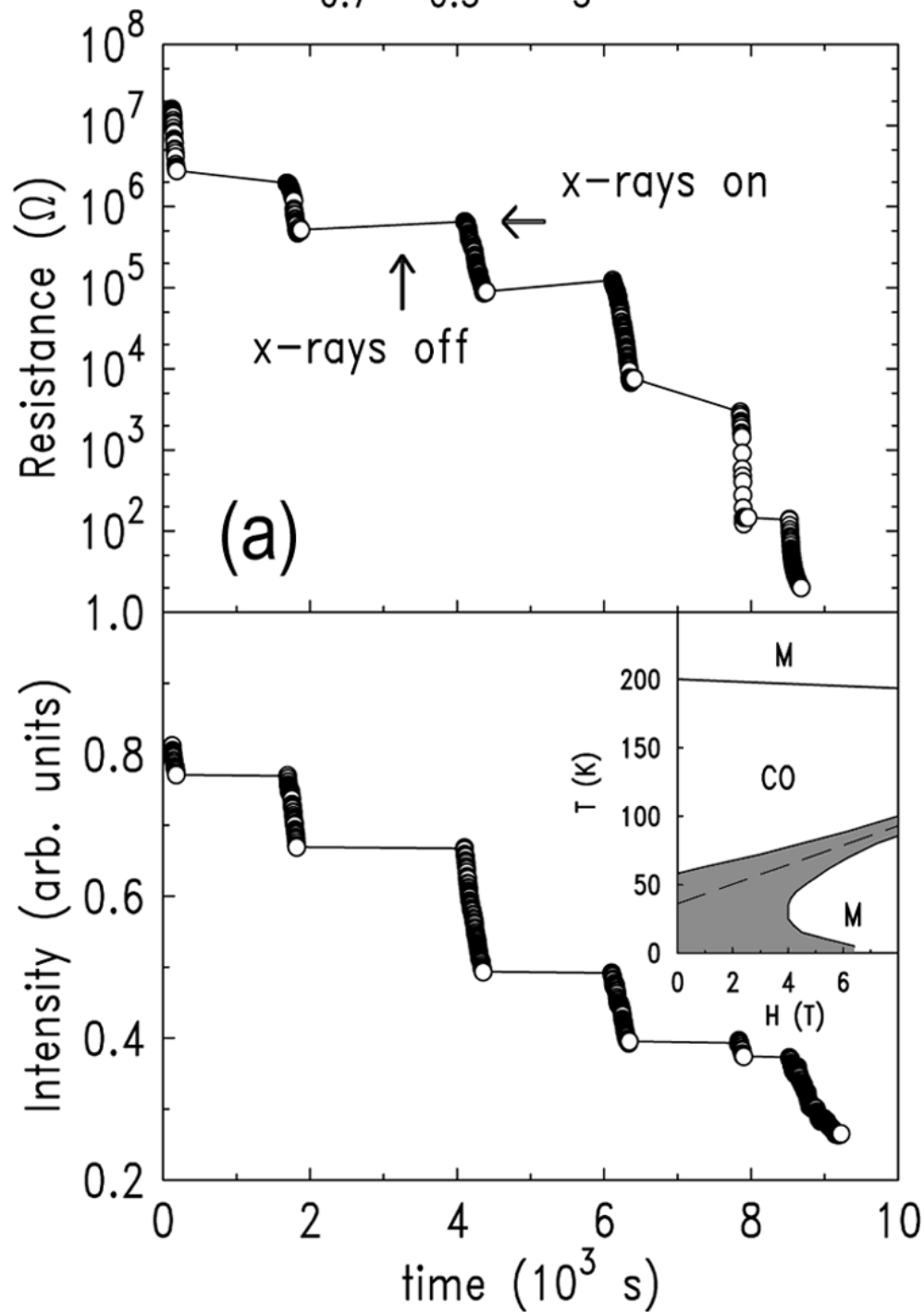
References

- [1] V. Kiryukhin *et al.*, Nature **386**, 813 (1997). See also D.E. Cox *et al.*, Phys. Rev. B **57**, 3305 (1998).
- [2] Y. Tomioka *et al.*, Phys. Rev. B **53**, R1689 (1996).
- [3] A. Asamitsu *et al.*, Nature **388**, 50 (1997).
- [4] K. Miyano *et al.*, Phys. Rev. Lett. **78**, 4257 (1997); M. Fiebig *et al.*, Science **280**, 1925 (1998).
- [5] Z. Jirak *et al.*, J. Magn. Magn. Mat. **53**, 153 (1985).
- [6] H. Yoshizawa *et al.*, Phys. Rev. B **52**, R13145 (1995).
- [7] Y. Tokura *et al.*, Phys. Rev. Lett. **76**, 3184 (1996).
- [8] D.V. Lang, in *Deep Centers in Semiconductors*, edited by S.T. Pantelides, (Gordon&Breach, New York, 1986), p. 489.
- [9] See, *e.g.*, M. Pollak and I. Riess, J. Phys. C **9**, 2339 (1976).
- [10] J.G. Simmons, J. Appl. Phys. **34**, 2581 (1963).
- [11] J.Z. Sun, Phil. Trans. Roy. Soc. A **356**, 1693 (1998).
- [12] In $\text{Pr}_{0.65}\text{Ca}_{0.245}\text{Sr}_{0.105}\text{MnO}_3$, some charge delocalization may take place in the barriers without a noticeable effect on the superlattice peak intensity (Fig. 1b), if this involves mostly Mn ions with local (incoherent or partially coherent) Jahn-Teller distortions.

Figure Captions

1. Electrical resistance and intensity of the (2, 1.5, 0) superlattice reflection characteristic of charge ordering as a function of x-ray exposure for (a) $\text{Pr}_{0.7}\text{Ca}_{0.3}\text{MnO}_3$ at $T=5\text{K}$, and (b) $\text{Pr}_{0.65}\text{Ca}_{0.245}\text{Sr}_{0.105}\text{MnO}_3$ at $T=100\text{K}$. The insets in the lower panels show the magnetic phase diagrams [2]. Significant hysteresis is observed in the shaded regions, and the dashed line represents the estimated thermodynamic phase boundaries following Ref. [7]. The inset in the upper right panel illustrates the experimental geometry.
2. Current-voltage characteristics of $\text{Pr}_{0.7}\text{Ca}_{0.3}\text{MnO}_3$ for (a) various x-ray exposures in zero field and (b) magnetic fields after a brief x-ray exposure (4.4×10^{12} photons/ mm^2), at $T=5\text{K}$. The curves in (a) are labeled by the incident x-ray fluence in units of 10^{13} photons per mm^2 incident on the sample. Those in (b) are labeled by the magnetic field in units of Tesla.
3. Temperature dependence of the current at a fixed voltage of 4V after a brief x-ray exposure (5.5×10^{12} photons/ mm^2). The data in the inset were measured at $H=2\text{T}$ after an exposure of 4.4×10^{12} photons/ mm^2 , the line is the Simmons tunneling expression [10] for two series junctions with barrier height 1.5 eV and thickness 15Å.
4. Typical current-voltage characteristics close to the percolation threshold of (a) x-ray generated and (b) magnetic field generated metallic clusters. The curves in (a) were taken sequentially at the same x-ray exposure (1.3×10^{14} photons/ mm^2), with the x-ray beam off. The curves in (b) were taken sequentially at a field of 3.75T, with the field on.

$\text{Pr}_{0.7}\text{Ca}_{0.3}\text{MnO}_3$ $T=5\text{K}$



$\text{Pr}_{0.65}\text{Ca}_{0.245}\text{Sr}_{0.105}\text{MnO}_3$ $T=100\text{K}$

